References

[1] B. C. DeLoach, Jr., "Radial-line coaxial filters in the microwave region," *IEEE Trans. Microwave Theory and Techniques*, vol. MTT-11, pp. 50–55, January 1963.

[2] J. R. Whinnery, H. W. Jamieson, and T. E. Robbins, "Coaxial-line discontinuities," *Proc. IRE*, vol. 32, pp. 695–709, November 1944.

[3] S. A. Schelkunoff, *Electromagnetic Waves*. Princeton, N. J.: Van Nostrand, 1943, sec. 8.6, pp. 267–272.

[4] N. Marcuvitz and J. Schwinger, "On the representation of electric and magnetic fields produced by currents and discontinuities in waveguides," *J. Appl. Phys.*, vol. 22, pp. 806–819, June 1951.

[5] R. E. Collin, *Field Theory of Guided Waves*. New York: McGraw-Hill, 1960, ch. 8.

[6] P. M. Morse and H. Feshbach, *Methods of Theoretical Physics*. New York: McGraw-Hill, 1953, sec. 9.4.

[7] G. N. Watson, *A Treatise on the Theory of Bessel Functions*. 2nd ed. London: Cambridge University Press, 1962, pp. 132–135, eqs. (2), (8), (11).

[8] L. Cairo and T. Kahan, *Variational Techniques in Electromagnetism*. Glasgow, Scotland: Blackie and Son, Ltd., 1965, ch. 4, sec. 2(a).

[9] J. M. Gelfand and S. V. Fomin, *Calculus of Variations*. Englewood Cliffs, N. J.: Prentice-Hall, 1963, ch. 8.

[10] G. L. Ragan, *Microwave Transmission Circuits*, M.I.T. Rad. Lab. Ser., vol. 9. New York: McGraw-Hill, 1948, pp. 146–147.

[11] H. Westphalen, "Koaxialleitungsfilter mit radialen Leitungen" (in German) *Archiv. Elect. Übertragung*, vol. 19, pp. 637–646, December 1965, and *Archiv. Elect. Übertragung*, vol. 21, pp. 52–60, January 1967. (These references were brought to the author's attention by H. Westphalen after this work had been completed.)

A Computer Designed, 720 to 1 Microwave Compression Filter

HARRY S. HEWITT, MEMBER, IEEE

***Abstract*—Compression filters with bandwidths up to 1000 MHz have application in high-resolution radar systems and rapid-scan receiver systems. A technique is presented for realizing a microwave linear delay (quadratic phase) versus frequency compression filter with sufficient delay accuracy to make compression ratios of up to 1000 to 1 feasible.**

The dispersive element in the compression filter is a silver tape with its broad side placed perpendicularly between the ground planes (instead of parallel, as in conventional stripline). The tape is folded back and forth upon itself in such a way that substantial coupling takes place between adjacent turns of the tape. A computer program has been written to determine the dimensions of the tape to achieve a linear delay versus frequency characteristic.

A folded tape compression filter was constructed with a differential delay of 1.2 μs over a bandwidth of 600 MHz centered at 1350 MHz giving a compression factor of 720 to 1. This filter was constructed in four identical sections, each section of which had a differential delay of 0.3 μs over the same bandwidth as the complete filter. The entire filter (four sections) occupies a volume about 16 by 4 by 5 inches. Measurement data are presented which illustrate that the desired accurate delay characteristic was realized to within the ±1 ns measurement uncertainty.

Introduction

In RECENT YEARS much attention has been focused on the use of pulse compression in "Chirp" radar systems. Typical pulse compression filters used in these systems have bandwidths of a few megahertz or less and differential time delays of up to several hundred microseconds. Somewhat less attention has been given to the development of radar and receiver systems using microwave compression filters, one reason probably being that no satisfactory tehnique for designing and constructing compression filters with bandwidths of hundreds of megahertz existed.

The pulse compression filter is a device for decreasing the time duration of, or compressing, a frequency modulated pulse of RF energy. This compressed pulse is used to improve the resolution or scan-rate capability of systems which use an RF pulse to indicate some parameter to be measured.

The search for devices which could be used to make microwave pulse compression filters has led investigators to study a variety of techniques. These include the dispersive helix;[1] the tapped delay line with tuned taps;[2],[3] the tapped delay line with broadband untuned taps;[4] first- and second-order, allpass quaterwave coupled transmission lines;[5] the yttrium-iron-garnet delay line;[6] and the folded tape meander line (FTML).[7] The FTML was chosen as a desirable structure for implementing a large time-bandwidth product compression filter because of its relatively easily predictable performance, its compact size, and its comparatively low cost.

The Folded Tape Meander Line

Fig. 1 shows the physical configuration of the FTML and defines the dimensions used in equations to follow. The meander line is totally immersed in dielectric; this assumption is maintained throughout the text of this paper. In practice, this is quite easy to accomplish; two sheets of dielectric

Manuscript received May 17, 1967; revised July 24, 1967.
The anthor is with the Systems Techniques Laboratories, Stanford, Calif.

material of thickness D separate the meander line from the ground planes above and below, and individual pieces of thickness S are cut to height W and a width L and are used to separate the meander line turns from each other. A strip of dielectric material of height W is placed along the length of the meander line on each side to complete the immersion.

The phase shift for each turn of the FTML (a turn is defined as a single piece of the conducting tape of width L within the periodic structures) is given implicitly by

$$\cot^2\left(\frac{\omega L}{2c}\right) = \frac{\gamma - \cos\theta - \gamma' \cos 2\theta + \cdots}{\gamma + \cos\theta - \gamma' \cos 2\theta + \cdots} \cot^2\left(\frac{\theta}{2}\right) \quad (1)$$

where

ω = radian frequency ($2\pi f$)
L = width of meander line ($L = \lambda_0/4$)
c = speed of light in the dielectric (meters per second)
γ, γ' = coupling parameters determined by dimensions S, B, W, and D
θ = phase shift at frequency ω (radians).

The time delay of an FTML turn is obtained by differentiating (1) with respect to θ to obtain $\tau = d\theta/d\omega$. If we define f_0 as the frequency for which L equals one-quarter wavelength, then $L = \lambda_0/4 = c/4f_0$.

In Fig. 2, the phase is plotted as a function of f/f_0 for three different values of the coupling parameter γ. The derivatives $d\theta/d\omega$ are plotted as time delay versus frequency (both normalized to f_0) in Fig. 3.

The coupling parameters γ, γ', etc., are defined as the ratios of the current on an FTML turn to the currents on the adjacent turns, the nearest nonadjacent turns, etc. Thus the coupling parameters can be related to the dimensions S, B, W, and D by computing these currents.

If it is assumed that a voltage V_n is applied to the nth conductor in an array, as shown in Fig. 4, and that all the other conductors in the array are at zero potential, then the coupling coefficients are defined in terms of the currents which flow on the array elements because of the presence of V_n. From Dunn,[7] we have

$$\gamma = -\frac{I_n}{2I_{n-1}}, \quad \gamma' = \frac{I_{n-2}}{I_{n-1}}, \quad \gamma'' = \frac{I_{n-3}}{I_{n-1}}, \text{ etc.} \quad (2)$$

These currents can be expressed in terms of the admittances Y_a, Y_b, and Y_c which relate the currents and voltages on the conductors for each of the three modes (a), (b), and (c) shown in Fig. 5. For example, the currents on the conductors in mode (a) are

$$I_n = I_{n+2} = I_{n+4} = I_{n-2} = I_{n-4} = \frac{V}{4} Y_a \quad (3)$$

$$I_{n-3} = I_{n-1} = I_{n+1} = I_{n+3} = -\frac{V}{4} Y_a. \quad (4)$$

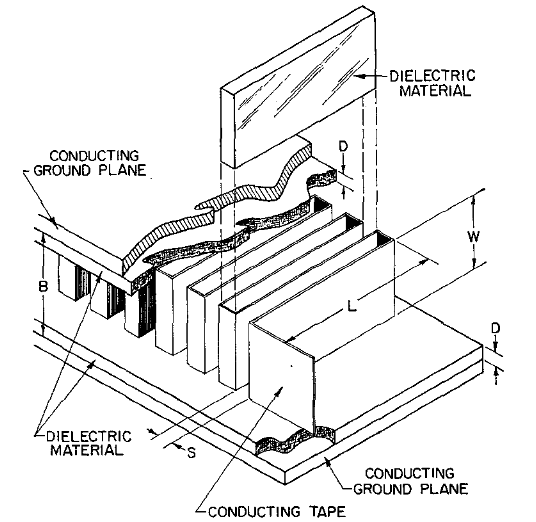

Fig. 1. FTML physical configuration.

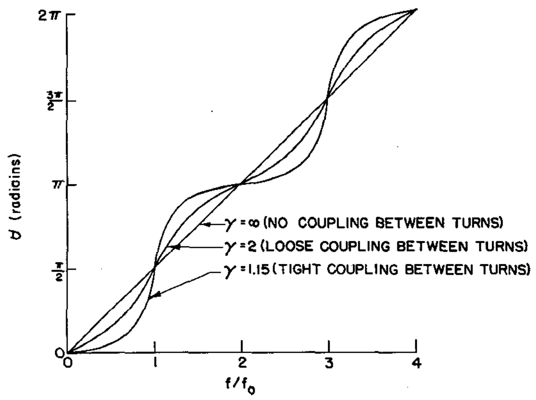

Fig. 2. Phase versus frequency for a single FTML turn.

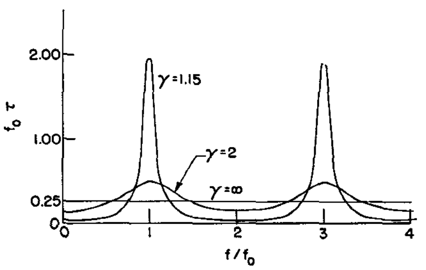

Fig. 3. Delay versus frequency for a single FTML turn.

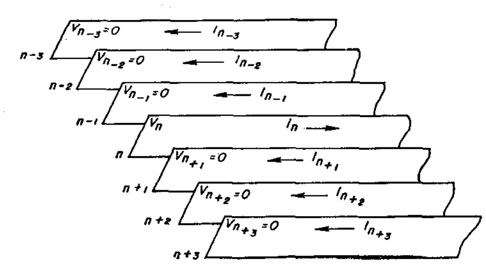

Fig. 4. Periodic array of conductors defining voltage and current relationships.

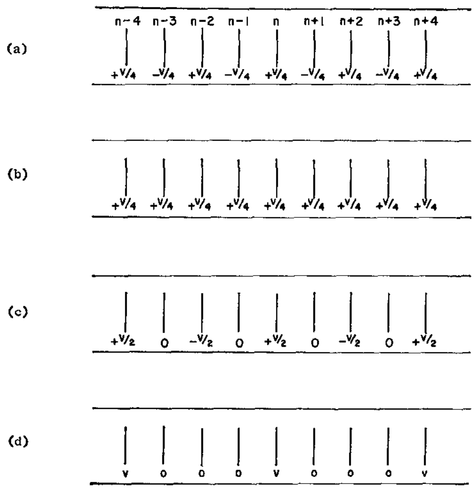

Fig. 5. Cross section of FTML array showing superposition of modes. Modes (a), (b), and (c) add to give (d).

The current on the FTML is the sum of the currents in each of the three modes.

$$I_n = \frac{V}{4} Y_a + \frac{V}{4} Y_b + \frac{V}{2} Y_c$$

$$= \frac{V}{4}(Y_a + Y_b + 2Y_c) \tag{5}$$

$$I_{n+1} = I_{n-1} = -\frac{V}{4} Y_a + \frac{V}{4} Y_b = \frac{V}{4}(Y_b - Y_a) \tag{6}$$

$$I_{n+2} = I_{n-2} = \frac{1}{2}\left[\frac{V}{4} Y_a + \frac{V}{4} Y_b - \frac{V}{2} Y_c\right]$$

$$= \frac{V}{8}(Y_a + Y_b - 2Y_c). \tag{7}$$

It follows that

$$\gamma = -\frac{I_n}{2I_{n-1}} = \frac{Y_a + Y_b + 2Y_c}{2(Y_a - Y_b)} \tag{8}$$

$$\gamma' = \frac{I_{n-2}}{I_{n-1}} = \frac{2Y_c - Y_b - Y_a}{2(Y_a - Y_b)}. \tag{9}$$

Assuming the elements of the array to be lossless TEM transmission lines, the admittances can be expressed in terms of the capacitance per unit length and the speed of light by the familiar equations

$$Y = \frac{1}{Z} = \sqrt{\frac{c_0}{l_0}} \tag{10}$$

$$c = \frac{1}{\sqrt{l_0 c_0}} \tag{11}$$

where

c = velocity of light in the dielectric (m/s)
l_0 = inductance per unit length (H/m)
c_0 = capacitance per unit length (F/m).

Combining (10) and (11),

$$Y = c_0 c. \tag{12}$$

The capacitances for the three modes of Fig. 5 can be obtained by means of the Schwartz-Christoffel transformation. The resultant expressions are

$$Y_a = \frac{\sqrt{\epsilon_r}}{30\pi} \frac{K(k_a')}{K(k_a)} \tag{13}$$

where

$$k_a' = sn\left[\frac{W}{B} K(k_1'), k_1'\right]$$

$$k_a' = \sqrt{1 - k_a^2}$$

$$\frac{K(k_1')}{K(k_1)} = \frac{B}{S}$$

ϵ_r is the relative dielectric constant.

$$Y_b = \frac{\sqrt{\epsilon_r}}{30\pi} \frac{K(k_b)}{K(k_b')} \tag{14}$$

where

$$k_b' = sn\left[\frac{2D}{B} K(k_1'), k_1'\right]$$

$$\frac{K(k_1')}{K(k_1)} = \frac{B}{S}$$

$$k_b' = \sqrt{1 - k_b^2}.$$

$$Y_c = \frac{\sqrt{\epsilon_r}}{30\pi} \frac{K(k_c')}{K(k_c)} \tag{15}$$

where

$$k_c' = sn\left[\frac{W}{B} K(k_1'), k_1'\right]$$

$$\frac{K(k_1')}{K(k_1)} = \frac{B}{2S}$$

$$k_c' = \sqrt{1 - k_c^2}.$$

In these expressions, $sn[u, k]$ is the Jacobian elliptic function with argument u and modulus k. $K(k)$ is the complete elliptic integral of the first kind. Fortunately, sufficiently good approximations to these relations exist so that it should never be necessary to use the exact expressions. From Dunn,[7] these approximations are

$$Y_a \cong \frac{\sqrt{\epsilon_r}}{30\pi}\left[\frac{W}{S} + \frac{2}{\pi}\ln 2 + \frac{1}{\pi}\ln\frac{1}{1 - 2e^{-2\pi D/S}}\right] \tag{16}$$

where $W/S > 1/2$, $D/S > 1/4$.

$$Y_b \cong \frac{\sqrt{\epsilon_r}}{30\pi}\left[\frac{1}{\frac{2D}{S} + \frac{2}{\pi}\ln 2 + \frac{1}{\pi}\ln\frac{1}{1-2e^{-\pi W/S}}}\right] \tag{17}$$

where $W/S > 1/2$, $D/S > 1/4$.

$$Y_c \cong \frac{\sqrt{\epsilon_r}}{30\pi}\left[\frac{W}{2S} + \frac{2}{\pi}\ln 2 + \frac{1}{\pi}\ln\frac{1}{1-2e^{-\pi D/S}}\right] \tag{18}$$

where $W/S > 1$, $D/S > 1/2$. It is interesting to note that, since the same term $\sqrt{\epsilon_r}$ appears in each of the admittance expressions, the coupling coefficients γ, γ', etc. are independent of the dielectric constant of the material surrounding the FTML. This is, of course, only true if the material is homogeneous and has the same dielectric constant throughout.

The relationships between γ and γ' and the ratio W/S are plotted in Figs. 6 and 7 for four values of D/S. It should be possible to construct an FTML to a delay accuracy of 1 percent by using the values of γ and γ' obtained directly from Figs. 6 and 7. If a higher degree of accuracy is necessary, the coupling coefficients should be calculated using (8) and (9).

Limitations imposed by the accuracy with which the dimensions can be realized will prevent γ'' and higher-order coupling coefficients from having a significant influence upon the delay of the FTML. The effect of γ' can be illustrated by calculating the maximum error one would encounter by ignoring this factor. The peak delay of an FTML turn occurs at a frequency $f = f_0$, where the phase shift through that turn is $\pi/2$ radians. Differentiating (1) with respect to θ, and then substituting $\theta = \pi/2$ into $d\theta/d\omega$, the peak delay is obtained. This is

$$\tau_{\text{peak}} = \frac{1}{4f_0}\,\frac{\gamma+\gamma'}{\gamma+\gamma'+1} \quad \text{(seconds)}. \tag{19}$$

The maximum delay error one would encounter by ignoring γ' in (19) is given by

$$\Delta\tau_{\text{peak}} = \frac{1}{4f_0}\left[\frac{\gamma}{\gamma-1} - \frac{\gamma+\gamma'}{\gamma+\gamma'-1}\right] \quad \text{(seconds)}. \tag{20}$$

The fractional error is

$$\frac{\Delta\tau_{\text{peak}}}{\tau_{\text{peak}}} = \frac{\left(\frac{\gamma'}{\gamma}\right)}{\gamma+\gamma'-1}. \tag{21}$$

The total delay of an FTML at a given frequency is the sum of all the component delays of each turn at that frequency. Fig. 8 illustrates how delay functions τ_1, τ_2, and τ_3, generated by FTML sections for which $f_0 = f_1, f_2$, and f_3, respectively, will add to give an overall delay characteristic, for the three cascaded sections, of $\tau_1+\tau_2+\tau_3$. The delay τ_k of any single section made up of n turns for which $f_0 = f_k$ will be directly proportional to n. Therefore, the synthesis of a desired delay function is accomplished by manipulating the number of FTML sections, the center frequency f_0 of each section, the number of turns in each section, and the values of γ, γ', etc. for each section.

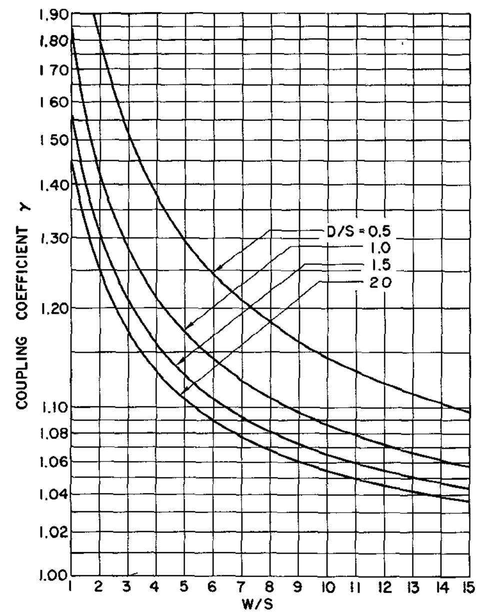

Fig. 6. γ versus W/S and D/S.

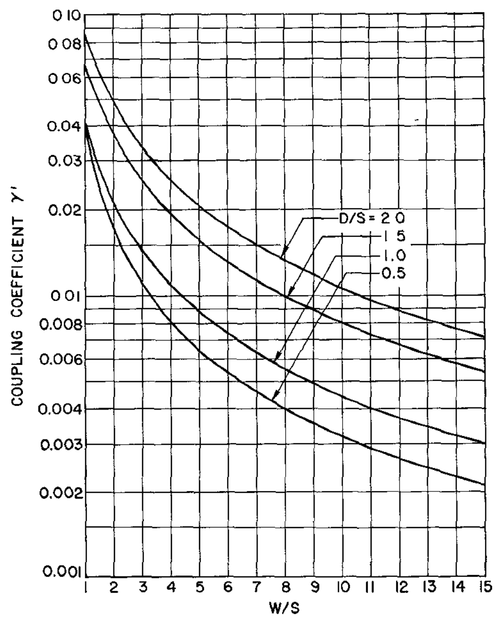

Fig. 7. γ' versus W/S and D/S.

For the generation of compression filter delay characteristics, the available degrees of freedom are more than necessary. It is usually sufficient to fix all parameters except the number of turns in each section. This requires, of course, that a sufficiently large number of sections be chosen to allow the desired delay characteristic to be generated within

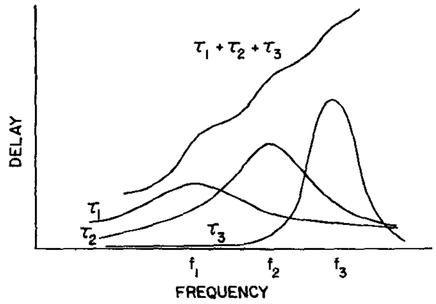

Fig. 8. Linear delay synthesis using 3 FTML sections.

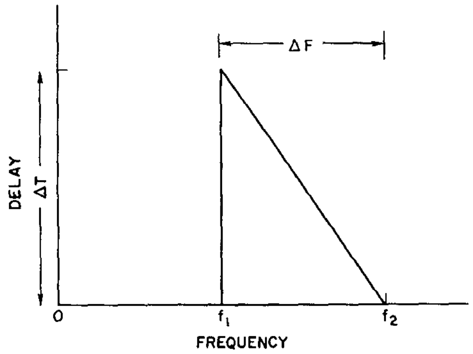

Fig. 9. Ideal compression filter with TBW $=\Delta T\ \Delta F$.

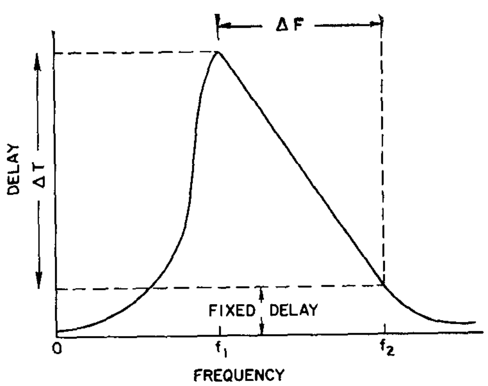

Fig. 10. FTML synthesized compression filter with TBW $=\Delta T\ \Delta F$.

the specified accuracy. The compression filter synthesis can be done without the aid of a computer, but it is not recommended. A computerized procedure is described later which will very accurately synthesize delay functions by manipulating the number of turns in each section of an FTML.

The approximate size of an FTML compression filter of a given time-bandwidth product (TBW) can be determined by considering the areas under the delay versus frequency curves. The area under the delay curve generated by a single-turn FTML can be obtained by integrating the delay function. Considering the frequency range from $f=0$ to $f=2f_0$ to be the range of interest, the area is

$$\text{Area} = \int_0^{2f_0} \tau df = \frac{1}{2\pi}\int_0^{2f_0} \frac{d\theta}{df} df = \frac{1}{2\pi}\int_0^{\pi} d\theta = \frac{1}{2} \cdot \quad (22)$$

It is seen that the FTML has a constant area under its delay function curve regardless of the values of γ, γ', etc. The area under the delay versus frequency curve of a compression filter with a given TBW is ideally TBW/2. Thus the minimum number of turns of an FTML required to synthesize such a delay function would be the area under the compression filter curve divided by the area under the curve for an FTML turn. This is $(\text{TBW}/2)\div\frac{1}{2}=\text{TBW}$ turns. In practice, all of the delay contribution of any given FTML turn cannot be contained between the frequency end points of the desired compression filter function, and also the synthesized delay function will always have some fixed delay because the delay of an FTML turn does not go to zero at $f=0$, $2f_0$, $4f_0$, etc. Thus the ideal compression filter delay curve of Fig. 9 will actually look like that of Fig. 10 when synthesized with an FTML. Fig. 10 shows that the area under the realizable compression filter curve is approximately double the area under the ideal curve. This suggests that approximately 2 TBW FTML turns would be required to synthesize a linear compression filter, and in practice this is the case. The use of a meander line with tighter coupling (smaller γ) would allow somewhat less than 2 TBW turns to be used, but the smaller number of turns is offset by the increased precision required of the various FTML dimensions.

The Computer Program

The computational program is designed to derive an FTML configuration to realize a desired delay versus frequency characteristic. This is accomplished by requiring the computer to determine the number of turns of conducting tape in each of M sections of FTML (each section being at a different center frequency f_0). The objective of the synthesis is to cause the composite delay characteristic of the M cascaded sections to equal the desired characteristic as nearly as possible. The accuracy with which the desired delay curve may be realized is related to the number of f_0s chosen, the values of γ and γ', the nature of the desired curve, and the amount of fixed delay[1] which can be tolerated. In general, the computer will be able to derive a compression filter characteristic which matches a desired characteristic to an accuracy which exceeds that with which the derived FTML can be realized because of dimensional accuracy limitations.

The program has been used exclusively to match delay characteristics in which delay varies linearly with frequency and in which the maximum delay occurs at the lowest frequency. This is a desirable configuration for a compression filter because the insertion loss, which in the FTML increases with increasing delay, is compensated to some extent by the fact that the FTML insertion loss also increases with increasing frequency for a given delay.

[1] In most cases, the computer will generate the desired delay function plus a constant delay which does not vary with frequency. It is this pedestal of constant delay, equivalent to a length of TEM transmission line, which is referred to as "fixed delay." See Fig. 10.

The program can be divided into three portions for analysis, and in operation the three portions are computed in the sequence given here.

Generation of Normalized Delay Function for Single FTML Turn

The input information necessary for this portion of the program includes the values of γ and γ', the number of different center frequencies f_0s which are to be used, and the frequency range over which the filter synthesis is to take place. This information is used to generate a normalized delay versus frequency function for a single FTML turn as shown in Fig. 3. This normalized function is then used to calculate all the possible values of f_{0T} which will be encountered at all possible values of f/f_0, and these values are stored in a two-dimensional matrix for use in the later portions of the program.

The Initial Approximation

This second phase of the synthesis program generates a set of ns which correspond to the number of turns at each value of f_0 and which will provide a delay function which is a rough approximation of the desired one. This is accomplished in the following manner:

1) The frequency range over which the f_0s are spread is divided into five intervals as shown in Fig. 11.

2) Within each of the five intervals, the composite delay at the center of the interval is calculated for one FTML turn centered at each of several f_0s in that interval.

3) The delays thus obtained are divided into the values of the desired delay function at the frequencies for which the delays were calculated. This yields a set of ns which, when truncated to integral numbers, form the number of turns for each of the FTML f_0s used in the initial approximation.

This approximate delay function is then used as the starting point for the third phase of the synthesis program.

The Error Reducing Process

In this final phase of the synthesis process, the delay curve that was generated as the initial approximation is subtracted from the desired curve to create an error function. From this point on, the object of the program is to reduce the peak-to-peak amplitude of this error function.

The locations of the original five intervals are discarded, and a new set of intervals is established which corresponds to the locations of the peaks and valleys in the error function. These peaks and valleys are located by moving a variable length sliding average along the error function from one end to the other. The sliding average is used so that minor fluctuations in the error function will not be treated as peaks or valleys. The initial sliding average uses 16 adjacent frequency points so as to locate gross peaks and valleys only, but as the error reducing process progresses, the sliding average must use progressively fewer numbers of points to pick out finer variations.

The initial intervals established in this portion of the program have their centers located approximately at the peaks

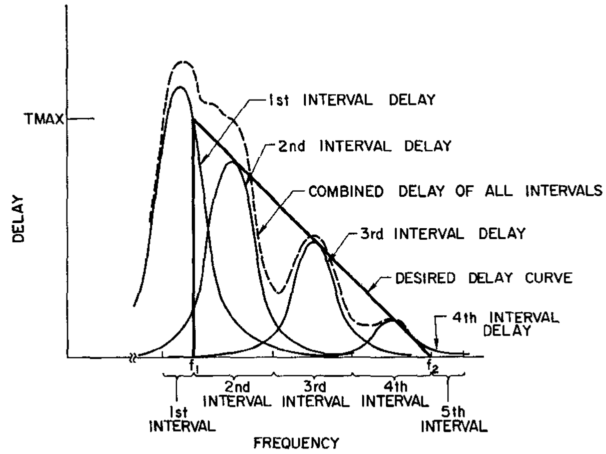

Fig. 11. Initial approximation to desired delay curve.

selected by the first peak–valley search. The boundaries of these intervals will then correspond approximately to the valleys. An appropriate number of turns is then subtracted near the centers of the peaks to bring the magnitude of the peaks down to a level corresponding approximately to the level of the nearest valley.

A new error curve is generated using the new values for the number of turns at each center frequency f_0. The process above is then repeated except that the intervals are centered on the newly found valleys, and turns are added instead of subtracted. This cycle (one subtraction routine plus one addition routine being one cycle) is repeated a number of times. Experience has shown that a solution accurate to a fraction of a percent with a given set of FTML variables is achieved after about fourteen cycles. Additional cycles are good insurance, however, since they require a running time of only a few seconds each (on an IBM 7090) and will show whether or not the computer has converged on an optimum solution.

Experimental Results

The procedure just described has been used to design and construct a compression filter for use in a Navy high-resolution radar-techniques investigation. The design goal for this filter was a differential delay of 1.2 μs varying linearly with frequency over the range from 1.05 GHz to 1.65 GHz.

The filter was constructed in four identical sections, each with a differential delay of 300 ns, varying from 390 ns at 1.05 GHz to 90 ns at 1.65 GHz. Fig. 12 is a photograph of one of the four sections with the upper dielectric sheet and ground plane removed to show the folded tape structure.

The measured insertion loss and delay versus frequency curves for one section are plotted point by point in Fig. 13. The size of the dots indicating the measured delay points is approximately representative of the measurement accuracy, and a straight edge will show that the delay error is less than ± 1 ns. A more descriptive picture of the delay accuracy is given in Fig. 14 which is a plot of the measured phase error obtained when the phase shift through the filter is subtracted from the ideal quadratic phase at each of the indi-

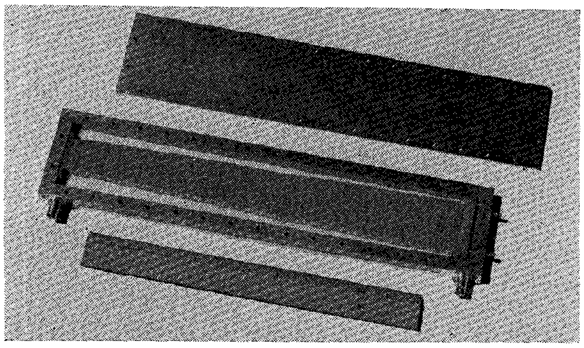

Fig. 12. Photograph of FTML structure.

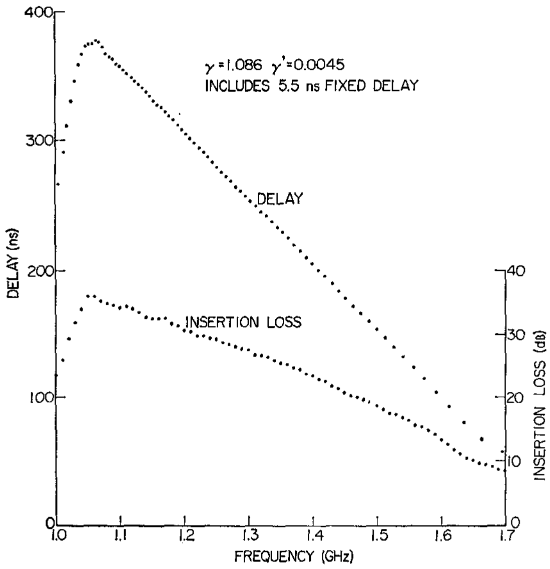

Fig. 13. Measured loss and delay versus frequency for one of the four compression filter sections.

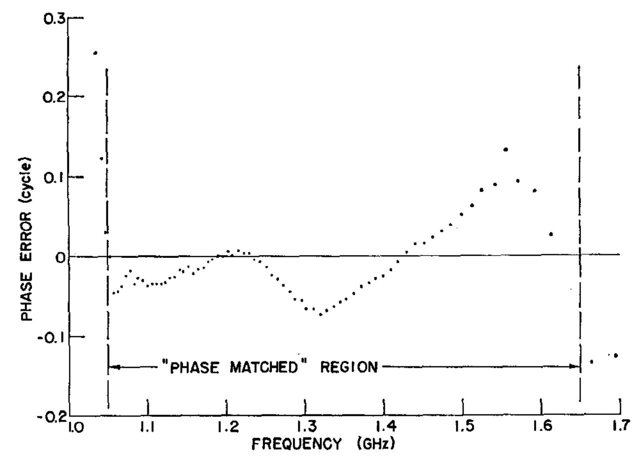

Fig. 14. Phase error versus frequency.

cated points. The phase shift through the filter changes by about 137 cycles in the 1.05 to 1.65 GHz frequency range, thus the maximum phase errors represent percentage errors of approximately ±0.1 percent over this frequency range.

The measured impedance, Fig. 15, shows that the FTML can easily be matched to a constant impedance system if VSWRs of 1.5 can be tolerated. No effort was made on the

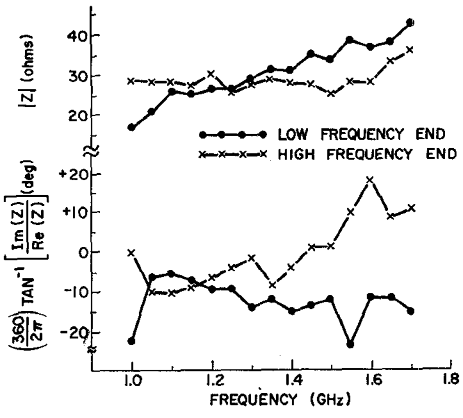

Fig. 15. Measured FTML impedance.

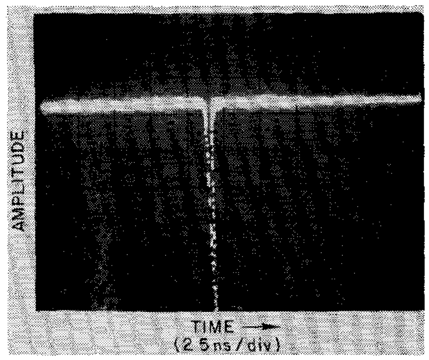

Fig. 16. Compressed pulse.

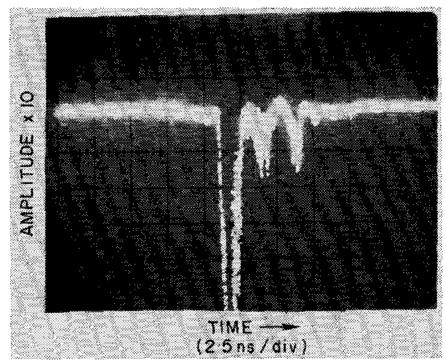

Fig. 17. Compressed pulse showing sidelobes (vertical scale expanded).

experimental filters to improve the impedance characteristics over those obtained initially, and it seems reasonable to expect that considerably lower VSWRs could be obtained if it should be necessary.

Figs. 16 and 17 are sampling oscilloscope photographs of the detected (square law) response of the compression filter section to a linearly scanning excitation. The filter was amplitude weighted with a Gaussian filter to a 3 dB bandwidth of approximately 250 MHz which yields a weighted compression factor of about 30.[2] The filter excitation is a 125 ns duration (between 3 dB points) FM pulse which is compressed to a duration of 4 ns by the filter. This rather heavy weighting

[2] The compression factor in this case is numerically equal to the filter bandwidth times the differential delay over that bandwidth. Thus $CF = (250\text{ MHz}) \times (125\text{ ns}) \cong 30$.

was chosen to show that the filter is capable of very good performance in terms of sidelobes. The expanded vertical scale of Fig. 17 proves the sidelobe levels to be lower than −30 dB. They actually may be lower than −40 dB because the two apparent sidelobes following the main compressed pulse at 25 ns intervals are not sidelobes but are internal reflections in the TWT amplifier used ahead of the oscilloscope as an aid to presentation.

Conclusion

The FTML technique appears well suited to a variety of problems requiring the generation of arbitrary, but continuous, delay characteristics over bandwidths of up to one octave. High losses and severe requirements on dimensional tolerances tend to limit the upper frequency range of usefulness of the technique to approximately 4 GHz. The lower-frequency limit is set by size and should be on the order of 100 MHz.

References

[1] V. E. Dunn, "A pulse compression filter employing a microwave helix," Stanford Electronics Labs., Stanford, Calif., Tech. Rept. 557-1, October 1960.

[2] H. S. Hewitt, W. R. Kincheloe, Jr., and M. H. Musser, "A study of several microwave compression filter techniques," Rome Air Development Center, Griffiss AFB, N. Y., Tech. Doc. Rept. RADC-TDR-64-398, November 1964.

[3] F. Mueller and R. Goodwin, "A wideband microwave compressive receiver," presented at IRE Internat'l Conv., New York, N. Y., March 26–29, 1962.

[4] H. S. Hewitt, "A design procedure for tapped-delay-line compression filters," Stanford Electronics Labs., Stanford, Calif., SEL-65-043 (TR1965-1), September 1965.

[5] "*Investigation of radar resolution and discrimination techniques*," Hazeltine Corp., Little Neck, N. Y., HRD Rept. 7816, December 1965 (Classified).

[6] J. H. Collins and G. G. Neilson, "Microwave pulse compression utilizing a yttrium iron garnet delay line," *Electronics Lett.*, vol. 1, p. 234, October 1965.

[7] V. E. Dunn, "Realization of microwave pulse compression filters by means of folded-tape meander lines," Stanford Electronics Labs., Stanford, Calif., SEL-62-113 (TR 557-3), October 1962.

Electromagnetic Resonances of Free Dielectric Spheres

MONIQUE GASTINE, LOUIS COURTOIS, AND JEAN LOUIS DORMANN

Abstract—**A systematic study is made of electromagnetic resonances of a spherical, free, and isotropic sample supposed to be without dielectric loss. The characteristic equation which is both complex and transcendant has been resolved with a computer. The results for the first modes (frequency and Q factor for ϵ varying between 1 and 100) are presented. The Q factor that is calculated represents the comparison between the energy stored by the resonance system and energy radiated per cycle; this is the theoretical maximum Q in the case of nonlossy materials.**

The different modes are classed in TE_{nmr} and TM_{nmr} modes which comprise exterior and interior modes. It is shown that for $n \geq r$ the energy is concentrated in all directions near the surface; these are known as surface modes. This systematic study is confirmed by experiments in which numerous modes have been observed and identified.

Introduction

The last few years have seen the publication of several studies of electromagnetic resonances of free dielectric samples. This is explained by the high Q factor that can be obtained with a small space factor, when using high-dielectric constant materials and a low dissipation factor tan δ. The resonators used lend themselves to a number of different applications. However, their use requires a good knowledge of their spectra and field configurations.

A systematic study has been made of the resonances of an isotropic spherical dielectric sample, supposed without loss, placed in an infinite medium. This problem had only, until now, been studied by approximating a high ϵ relative dielectric constant.[1]–[6]

Manuscript received May 18, 1967; revised July 31, 1967.

The authors are with the Laboratoire de Magnetisme et de Physique du Solide, Centre National de la Recherche Scientifique, Bellevue, France.

Characteristic Equation

The dielectric sample creates in its proximity a concentration of semistationary electromagnetic energy. By using the Bromwich method, Maxwell's equations have been resolved taking into account the boundary conditions, zero energy at infinity. By using the spherical coordinates (ρ, θ, ϕ) it has been possible to class the waves as transverse electric modes (TE) and transverse magnetic modes (TM).

For a TE mode on the inside of the sample, the fields are